Assessment of Seasonal Variation of Land Surface Temperature (LST) in an Urban Area

Arun Mondal[1], Deepak Khare[2], Sananda Kundu[3], Prabhash Kumar Mishra[4],

ABSTRACT - Land surface temperature varies with different landuse category. Thermal infrared (TIR) remote sensing technique is able to identify the temperature as measured at the time of satellite overpass. The present study is an attempt to find the seasonal variation of temperature in different landuse pattern and management in Delhi city. Land surface temperature has been calculated from Landsat TM5 satellite images in different seasons (January, April, June and October) by Mono-window algorithm. Field validation of same season (June) has been carried out with calculated temperature which varies from 0.5ºC to 1.8ºC. Landuse map has been classified into five major classes (Built-up, Dense vegetation, Light vegetation, water body and fallow land) by supervised Fuzzy C-mean method with 88% overall accuracy. Finally, the results indicate that LST of vegetation and water is much low in comparison to others. The difference in LST can be minimized in highly heated areas by initiating plantation programmes in the city built up areas and surroundings throughout the year.

Keywords: Delhi, Landsat TM, Land Surface Temperature, Seasonal Variation,Thermal infrared

1.0 Introduction:

Extreme heat in the urban areas is the major trouble at the present day consequence of global warming. *Manley (1958)* proposed the Urban Heat Island (UHI) in the early 19th century. *Miller and Small (2003)* have noticed that fast expanding cities pose environmental challenge in this century and it requires analytic approaches and latest sources of information and data. It is found that about 48% of the world populations living in urban areas are exposed to urban heating problems. In future more people will be susceptible to this problem as people residing in urban areas are suppose to grow to five billion by 2030 *(World Urbanization Prospectus, 2003)*. According to *Memon et al. (2008)* urban heat island is the result of many man-made and natural factors.

Number of researchers have studied relation between the land surface temperature and plant cover in various areas by using satellite images, and have found the result to be negative (*Weng, 2004; Yang et al, 2006; Jiang et al, 2006*). Some other studies with respect to the relationship between impervious surface of land and LST were done to study urban heat island (*Yuan and Bauer, 2007*) and some researchers have used remote sensing to achieve this (*Lu and Weng, 2004; Lu and Weng, 2006*). UHIs develop when a large portion of the natural land-cover or vegetation are replaced by the built surface that trap the incoming solar radiation at the day time and re-radiate it at night (*Oke, 1982*). Thermal remote sensing is used extensively for the analysis of the temperature change. *Voogt and Oke (2003)* used the thermal remote sensing in urban areas for the assessment of urban heat island. Change in the landscape of city areas increase the temperature and have effect on the local atmosphere. Variation in thermal condition has effect on different species and vegetation causing change in ecology and environment *(Knapp et al., 2008; Shustack et al., 2009)*. According to *Stott et al., (2004)* and *Fouillet et al., (2006)*, increasing danger of illness like hyperthermia, heat strokes etc. are occurring more due to increase in heat wave in the urban areas.

Environmental problems like assessment of the changing land surface temperature can be dealt with thermal remote sensing which can give some effective results regarding the present position of the city. In the present study, seasonal temperature variation of different landuse of Delhi city has been assessed with the help of Landsat TM data for 2011. Validation of LST of June, 2010 was done which also shows higher temperature distribution during summer in the built-up areas.

2.0 Study Area:

Delhi is the capital of India located between 28º23'17''N and 28º53'00''N latitude, and 76º50'24'' E and 76º20'37''E longitude. It covers an area of about 1483 km² and has a population of around 16 million (2011 census). The city is located on the bank of river Yamuna and is bounded by the states of Uttar Pradash on the east and Haryana on the north, south and west. The climate is semi-arid in nature with high range of temperature. In June it is 48°C and in December it is about 3°C. The climate also has low rainfall intensity (annual average rainfall 60mm). Delhi experiences very hot summer and cold winter (Fig.1).

[1,3,4] *Research Scholar, Department of Water Resources Development and Management,*
Indian Institute of Technology Roorkee, Roorkee (U.A.), India,
[2] *Professor, Department of Water Resources Development and Management,*
Indian Institute of Technology Roorkee, Roorkee (U.A.), India,
[1]*arun.iirs@gmail.com;* [2]*kharefwt@gmail.com;* [3]*sanandakundu@gmail.com;*
[4]*erprabhash@gmail.com;*
Corresponding Author : [1]*arun.iirs@gmail.com*

3.0 Data and Methods:

Data used in the study are given in Table1.

The data was geo-referenced with Universal Transverse Mercator (UTM) projection and WGS84 Datum and supervised Fuzzy C mean was used for the classification of the image. Atmospheric correction was also applied on the data. Image calibration was done by conversion of uncalibrated Digital Number (DN) to the calibrated radiance. Then it is changed into spectral reflectance. Land surface temperature (LST) was computed from the DN value of satellite image (Landsat TM5). DN value was converted into the spectral radiance (L_{TOA}) by using the official ranges approved from NASA for $L\max_{\lambda}$ and $L\min_{\lambda}$ *(Chander and Brian, 2003; NASA, 2004*).

Estimation of the upwelling radiance and atmospheric transmission were generated by the web-based results provided by NASA *(Barsi et al., 2005)*.

$$L_{TOA} = \tau\varepsilon L_T + L_u^{\uparrow} + \tau(1-\varepsilon)L_d^{\downarrow} \qquad (1)$$

L_{TOA} = TOA radiance measured by the instruments

$L_u^{\uparrow}$ = Upwelling

$L_d^{\downarrow}$ = Downwelling

ε = Emissivity

τ = Atmospheric Transmissivity

Here T represents the temperature in Kelvin; L_λ stands for the spectral radiance in $W/m^2sr^{-1}\mu m^{-1}$, and k_1 and k_2 are considered as the calibration constants

$$T = \frac{K_2}{\ln(\frac{K_1}{L_T}+1)} \qquad (2)$$

L_T = Radiance band 6 (W/m2 ·sr ·μm)

T = Brightness temperature (Kelvin)

K1 = Constant 1 (W/m2 ·sr ·μm)

K2 = Constant 2 (Kelvin)

4.0 Results and discussion:

The image of 22nd June, 2010 of Landsat TM data was digitally classified in to five classes of built-up area, water body, dense vegetation, light vegetation and fallow land (Table 2). Built-up area extends over 685 km^2 constituting about 46.23% of the total area. Other types of landuse are found in the north, south and southwestern parts. Water body covers about 8 km^2 area, dense vegetation with 65.84 km^2 of area, light vegetation with 496 km^2 area and fallow land with about 226 km^2 area (Table2). The landuse map is given in Fig.2.

4.1. Analysis of Emissivity for various seasons

Emissivity determines the absorbed quantity of heat by the object. 29th January, 2010 (Fig. 3) represents the winter, when emissivity was more than 0.98 in most of the area. Built-up area has emissivity of more than 0.98 and thus indicates high absorption of solar energy. Vegetation in some parts represents less emissivity of 0.93 to 0.96. Emissivity of 3rd April, 2010 is less with the built-up areas having more than 0.98 emissivity. The water bodies and vegetation represent less emissivity. June 22nd, 2010 represent high emissivity of more than 0.98 in most of the region. Only few areas with vegetation and water in the river have low emissivity. June is the summer month and thus is very hot absorbing maximum energy. October 12th, 2010 shows high emissivity of more than 0.98 in the built-up areas. Other parts have less emissivity particularly vegetation and water bodies. Thus, from the maps it is evident that built-up areas emit much more heat than other landuses like vegetation and water bodies.

4.2 Land Surface Temperature

The LST of June shows mean temperature of the built-up area around 40.42°C while the range varies from 38 to 42 °C. Fallow lands also have very high temperatures as they are open lands and absorbs heat. The water bodies and dense vegetation represent much less temperature of around 31 °C and 28 °C respectively. Therefore areas with water bodies and vegetations have comparatively cooler atmosphere. Light vegetation or cultivable lands have average temperature of about 38 °C in June. In October, mean temperature of built-up area is about 34 °C and for dense vegetation and water body it is 28°C and 26°C respectively. For January, which is a winter time, the temperature remains low for all the landuse classes in comparison to other seasons. Built-up area signifies about 14°C while dense vegetation and water body have 11°C and 13°C respectively. April has moderate temperature for built-up areas around 22°C. Vegetation and water body have lower temperature of 16°C and 15°C respectively in April (Table3). In all these seasons, fallow lands also depict high temperature in summer months after the built-up areas. LST of 22nd June was validated with the field survey during that day with the infrared thermometer. The maps of LST of four seasons are given in Fig. 4.

Graphically the LST of different landuse in different seasons are given in Fig. 5 where fallow land and built-up have higher temperatures especially during summer. So places around these landuse classes remain very hot in summer. But in winter, fallow lands have less temperature than built-up and light vegetation as they release heat quickly.

5.0 Conclusions:

Thermal remote sensing was used in the study for the analysis of Land Surface Temperature (LST). Change in temperature with the seasons with different landuse was considered for this study. Urban environment is a major concern nowadays with the increasing threat of global warming. TIR sensors with global imaging capacity are helpful for obtaining the LST. Landsat TM was used in the present work which was classified in to five classes. The overall accuracy achieved in the classification procedure was 88%. Four seasons of summer, autumn, winter and spring were considered for the analysis and it was found that the

water bodies and vegetation have much less temperature than the built-up areas and fallow lands in summer. Thus to reduce the urban heat in summer, some management strategies should be taken by increasing the plantations and ponds in the built-up area. Fallow lands should also be taken in to care as they are sources of higher temperature in summer and lower temperature in winter.

References

1. Barsi, J.A., Schott, J.R., Palluconi, F.D. Hook, S.J., 2005. Validation of a Web-Based Atmospheric Correction Tool for Single Thermal Band Instruments. Earth Observing Systems X, edited by James J. Butler, Proceedings of SPIE Vol. 5882 (SPIE, Bellingham, WA, 2005) 0277-786X/05/$15 · doi: 10.1117/12.619990.
2. Chander, G., Brian, L.M., 2003. Revised Landsat-5 TM Radiometric Calibration Procedures and post-calibration Dynamic Ranges. IEEE Transactions on Geosciences and Remote Sensing, 41 (11), 2674-2677.
3. Fouillet, A., Rey, G., Laurent, F., Pavilion, G., Bellec, S., Guihenneuc-Jouyaux, C., et al., 2006. Excess mortality related to the August 2003 heat wave in France. Int. Arch. Occ. Environ. Health 80: 16–24.
4. Jiang, Z.Y., Chen, Y.H., Li, J., 2006. Heat Island Effect of Beijng Based on Landsat TM Data. Geomatics and Information Science of Wuhan University. 31 (2), 120–123.
5. Knapp, S., Kuhn, I., Schweiger, O., Klotz, S., 2008. Challenging urban species diversity: contrasting phylogenetic patterns across plant functional groups in Germany. Ecol. Lett. 11, 1054–1064.
6. Lu, D., Weng, Q., 2004. Spectral mixture analysis of the urban landscape in indianapolis with Landsat ETM+ imagery. Photogrammetric Engineering and Remote Sensing 70, 1053-1062.
7. Lu, D., Weng, Q., 2006. Use of impervious surface in urban land-use classification. Remote Sensing of Environment 102, 146-160.
8. Manley G., 1958. On the frequency of snow fall in metropolitan England. Quart J Roy Meteor Soc. 84 (359):70–72.
9. Memon, R.A., Leung, D.Y.C., Liu, C.H., 2008. Impacts of important environmental variables on the urban heating. Climate change and Urban Design Conference, Oslo, Norway. 14–16 September 2008.
10. Miller, R.B., Small, C., 2003. Cities from space: potential applications of remote sensing in urban environmental research and policy. Environmental Science & Policy 6, 129–137.
11. NASA. 2004. Landsat Project Science Office. Landsat 7 Science Data Users Handbook. Chapt. 11 Data Products.
12. Oke, T., 1982. The energetic basis of urban heat island. Journal of Meteorological Society 108 (455), 1-24.
13. Shustack, D.P., Rodewald, A.D., Waite, T.A., 2009. Springtime in the city: exotic shrubs promote earlier greenup in urban forests. Biol. Invasions 11, 1357–1371.
14. Stott, P.A., Stone, D.A., Allen, M.R., 2004. Human contribution to the European heat wave of 2003. Nature. 432: 610–614.
15. Voogt, J.A., Oke, T.R., 2003. Thermal remote sensing of urban climates. Remote Sensing of Environment 86, 370–384.
16. Weng QH. 2004., Estimation of land surface temperature–vegetation abundance relationship for urban heat island studies. Remote Sensing of Environment. (89):467–483
17. World Urbanization Prospectus, The 2003 Revision, 2004. Department of Economic and Social Affairs, Population Division. United Nations, New York.
18. Yang, Y.B., Su, W.Z., Jiang, N., 2006. Time-Space Character Analysis of Urban Heat Island Effect in Nanjing City using Remote Sensing. Remote Sensing Technology and Application. 21(6), 488–492.
19. Yuan, F., Bauer, M., 2007. Comparison of impervious surface area and normalized difference vegetation index as indicators of surface urban heat island effects in Landsat imagery. Remote Sensing of Environment 106, 375-386.
20. Yuan, F., Bauer, M., 2007. Comparison of impervious surface area and normalized difference vegetation index as indicators of surface urban heat island effects in Landsat imagery. Remote Sensing of Environment 106, 375-386.

Table1 Data

SERIAL NO.	SENSOR TYPE	AQUIRED DATE	RESOLUTION (m)	
			Band no:1, 2, 3, 4, 5, 7	Band no: 6
1	Landsat TM	29.01.2010	30	60
2	Landsat TM	03.04.2010	30	60
3	Landsat TM	22.06.2010	30	60
4	Landsat TM	12.10.2010	30	60

Table 2 Landuse/ Land cover Classes

Serial Number	Land cover classes	Area (km^2)	Area (%)
1	Built-up area	685.53	46.23
2	Light Vegetation	496.56	33.48
3	Dense Vegetation	65.84	4.44
4	Water Body	8.96	0.60
5	Fallow land	226.11	15.25
	Total	1483.00	100.00

Table3 Statistics of LST in four seasons

Landuse	Date	Mean (°C)	Median (°C)	Mode (°C)	Minimum (°C)	Maximum (°C)	Standard Deviation
Water bodies	Jan	13.01	13.74	13.50	11.52	15.23	0.63
	April	15.94	15.85	16.34	12.52	18.65	0.93
	June	31.31	31.11	30.42	29.72	35.18	0.99
	Oct	26.32	26.20	25.81	24.45	29.56	0.91
Built-up area	Jan	14.62	14.25	14.32	13.15	16.36	0.62
	April	22.52	22.65	21.86	17.03	25.05	0.66
	June	40.42	40.43	40.43	38.49	42.36	0.68
	Oct	34.75	34.77	34.77	26.30	37.30	0.84
Dense vegetation	Jan	11.81	11.05	14.85	7.96	15.05	2.06
	April	16.94	17.23	18.95	12.11	19.98	1.51
	June	28.17	27.34	33.84	23.78	37.83	2.87
	Oct	28.12	28.82	30.22	21.20	32.19	2.36
Light vegetation	Jan	13.97	14.52	14.35	7.66	18.36	2.60
	April	18.80	18.68	23.86	13.95	24.65	2.25

	June	34.97	35.23	36.39	25.23	38.12	1.87
	Oct	30.43	31.63	32.34	22.55	35.14	3.19
Fallow land	Jan	13.01	13.74	13.50	11.52	15.23	0.63
	April	15.94	15.85	16.34	12.52	18.65	0.93
	June	31.31	31.11	30.42	29.72	35.18	0.99
	Oct	26.32	26.20	25.81	24.45	29.56	0.91

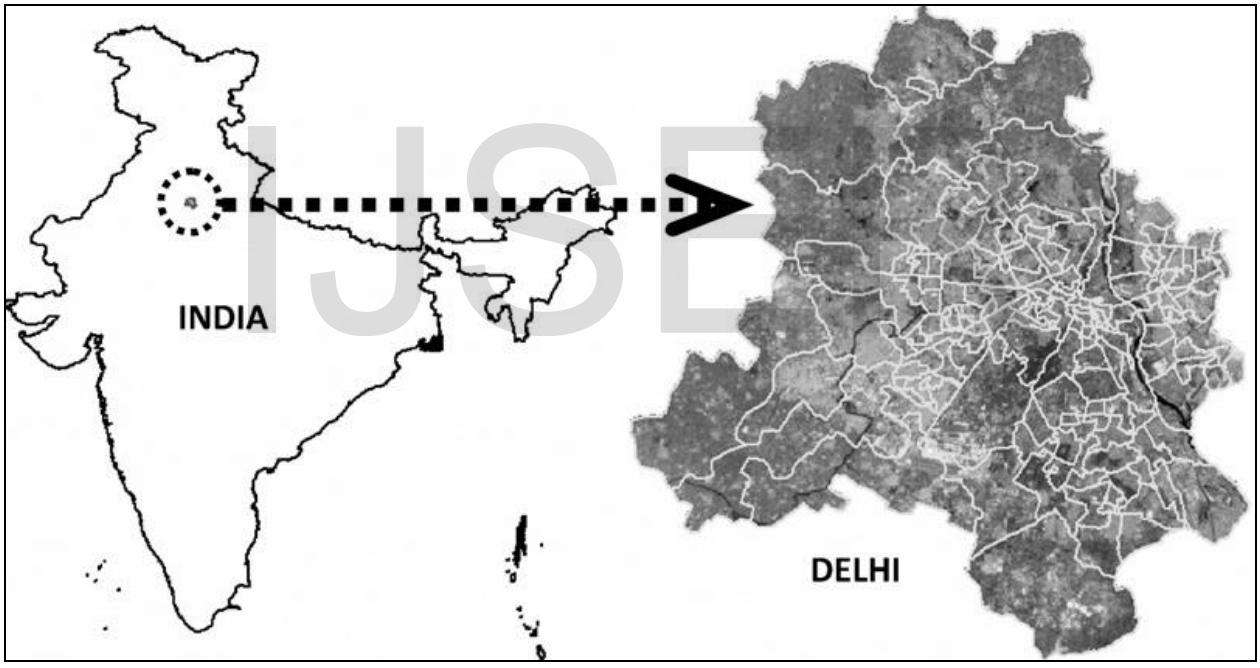

Fig.1 Study area

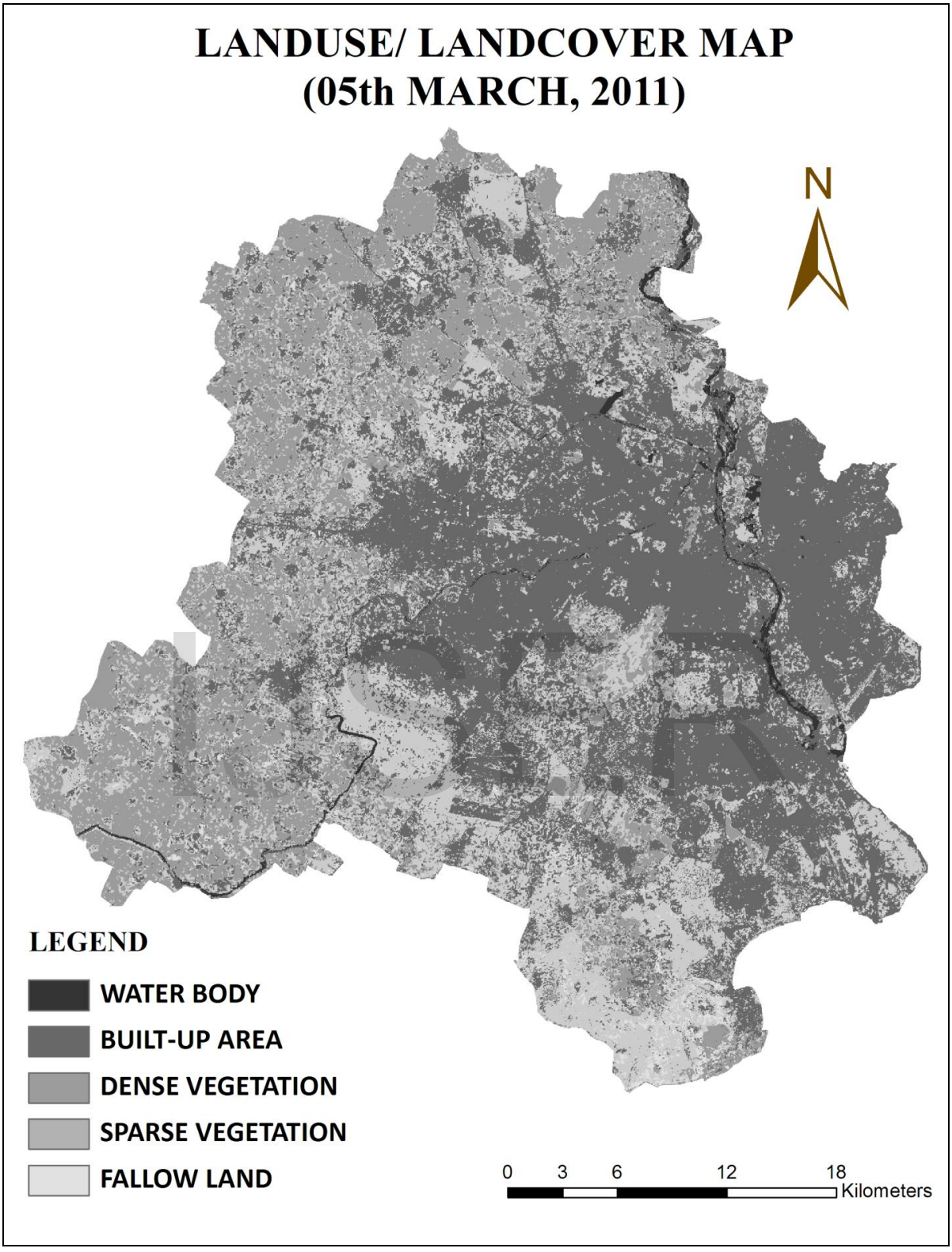

Fig.2 Landuse

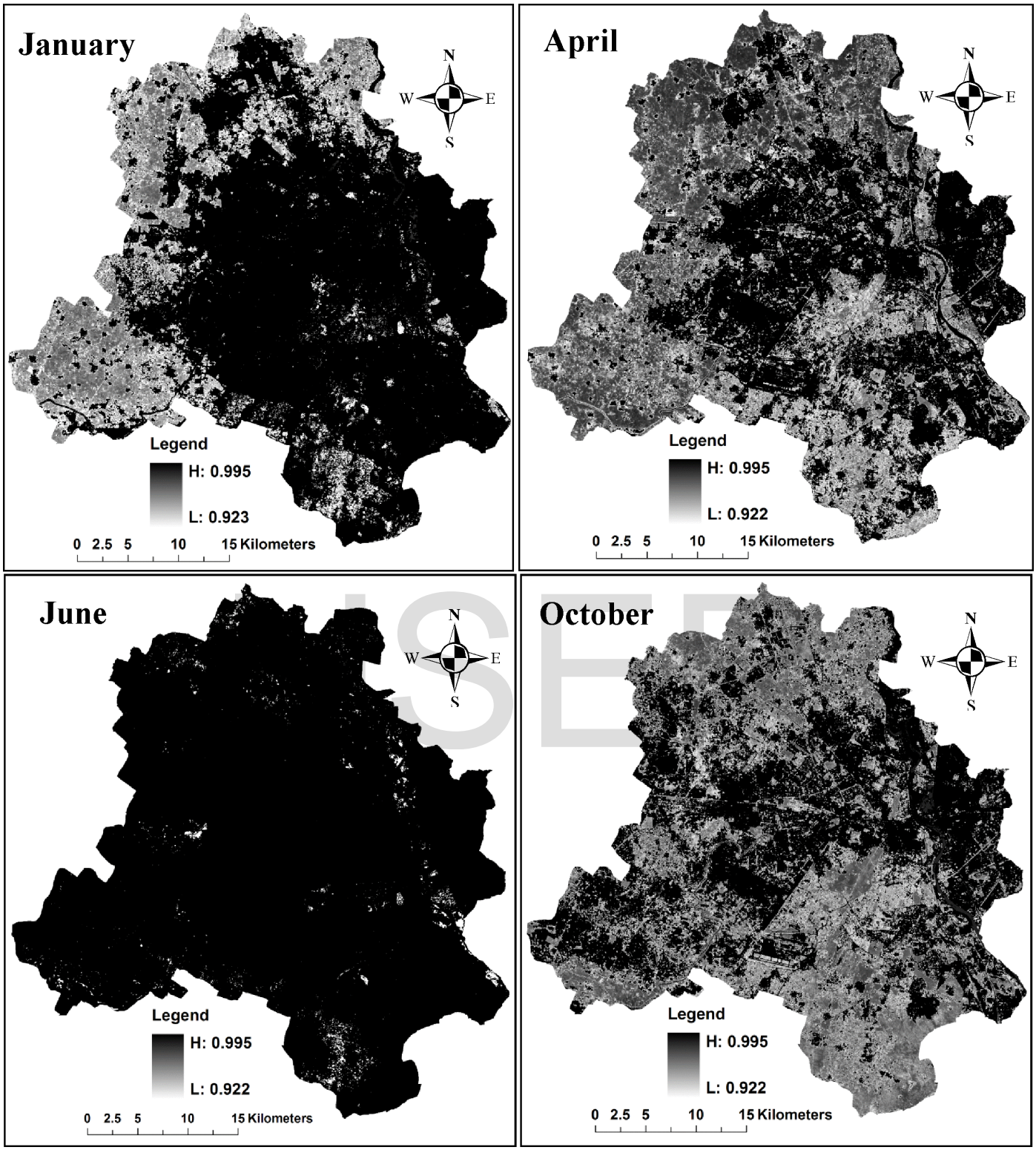

Fig.3 Emissivity

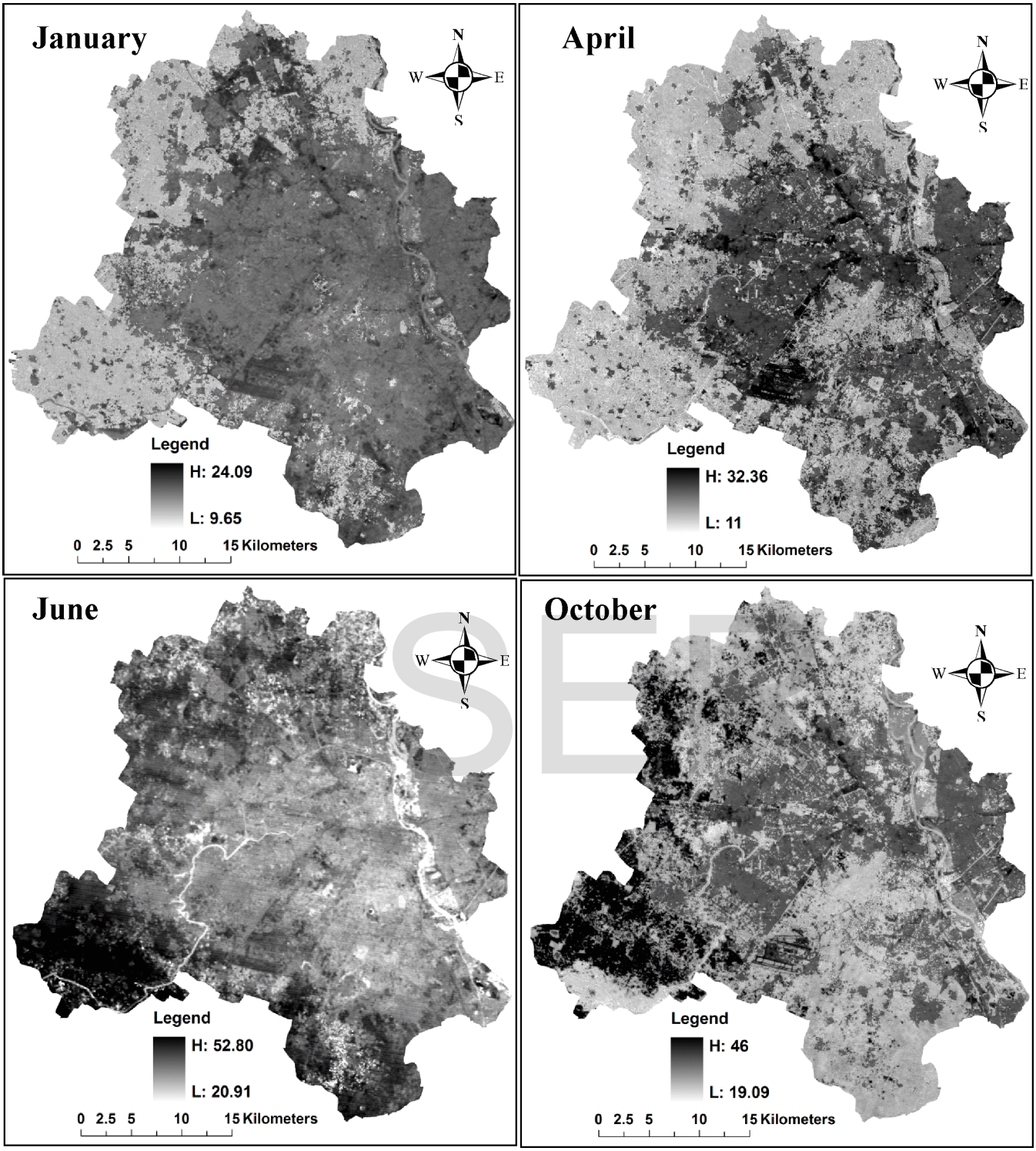

Fig.4 Land Surface Temperature